# An extension of the Generalized Actuator Disc Theory for aerodynamic analysis of the diffuser-augmented wind turbines

Liu, Yingyi
Interdisciplinary Graduate School of Engineering Science, Kyushu University

Yoshida, Shigeo
Research Institute for Applied Mechanics, Kyushu University



出版情報：Energy. 93 (2), pp.1852-1859, 2015-12-15. Elsevier
バージョン：

# An extension of the Generalized Actuator Disc Theory for aerodynamic analysis of the diffuser-augmented wind turbines

*Yingyi Liu*[1,*], *Shigeo Yoshida*[2]

[1]Interdisciplinary Graduate School of Engineering Science, Kyushu University, Kasuga, Fukuoka 816-8580, JAPAN

[2]Research Institute for Applied Mechanics, Kyushu University, Kasuga, Fukuoka 816-8580, JAPAN

---

## Abstract

The one-dimensional momentum theory is essential for understating the physical mechanism behind the phenomena of the DAWT (Diffuser-Augmented Wind Turbines). The present work tries to extend the existing GADT (Generalized Actuator Disc Theory) that proposed by Jamieson (2008). Firstly, the GADT is modified to include an effective diffuser efficiency, which is affected by the thrust loading or axial induction. Secondly, Glauert corrections to the DAWT system in the turbulent wake state are proposed, modelled by a linear and a quadratic approximation, respectively. Finally, for prediction of the axial velocity profile at rotor plane bearing various thrust loadings, an empirical model is established, which can be further used to predict the diffuser axial induction. In addition, the 'cut-off point' in Glauert correction and the 'critical thrust loading' in axial velocity profile prediction are newly defined to assist the analysis. All the above formulations have been compared and validated with Jamieson's results and Hansen's CFD data, justifying the effectiveness of the present model.

*Keywords*: Momentum theory; Diffuser-augmented; effective diffuser efficiency; Glauert correction; velocity speed-up ratio

---

## 1 Introduction

It has long been pursued by the people around the world for energy extraction concepts with their efficiency as high as possible, among which the DAWT (Diffuser-Augmented Wind Turbines) can be viewed as one of those innovative technologies. With shrouding of the diffuser, DAWT may be

[*] Corresponding author. Tel.: +81-080-8565-7934.
E-mail address: liuyingyi@riam.kyushu-u.ac.jp

capable of exceeding the Betz limit (e. g. Oka et al. [1]), which has been usually considered as the limit of power performance coefficient of the bare wind turbines.

Many investigations have been done on DAWT technology on various aspects, which have been lasted over 50 years. Lilley and Rainbird [2] discovered that the increase in axial velocity and the reduction of blade tip losses might be the main factors for the additional power augmentation from a duct. Experimental studies later performed by Gilbert & Foreman ([3], [4]) and Igra [5], showing that power extraction beyond the Betz limit was possible. At the same time, Fletcher [6] attempted to develop a computational analysis method, based on coupling his momentum theory with the Blade Element Method. Dick [7] proved that for a mass concentrator similar to DAWT, the power coefficient of the system can be written as the product of a mass concentration coefficient and an extraction coefficient. Thereafter, the research on DAWT had been suspended for almost 20 years partly due to the technology had not been considered profitable relatively to conventional wind turbines at that moment. Relevant researches boomed again till the beginning of the 21$^{st}$ century, while Hansen et al. [8] simulated a diffuser which was made from deforming NACA0015 aerofoil by the CFD software *EllipSys*. Later, Van Bussel [9] first introduced the back pressure velocity ratio and showed that the power augmentation could be achieved by increasing the exit area ratio which leads to an under pressure at the nozzle. Jamieson ([10], [11], [12]) developed a generalized limit theory for the shrouded wind turbine through new formulations, aiming at its application to a DAWT BEM (Blade Element Method) code which was implemented in the wind turbine design software package *Bladed*. In short, until recently, the methodologies for investigating DAWT have mainly three branches, the computational (CFD) method, the theoretical (empirical) method and the experimental method, which have been all performed in the history.

As known by all, for the design purpose, it is necessary to develop a fast and accurate method, in order to reduce the economic cost and the labour force. Therefore, we are always trying not to

depend on experiment or CFD too much. The theoretical method provides a best solution taking into account both the cost and the efficiency, as long as the accuracy is guaranteed. The theoretical model for DAWT has evolved into several versions based on the understanding of the physical mechanism for the augmentation, among which Jamieson's formulation looks more comprehensive, since it has already been designed to cover the previous models at the beginning. Other's experimental results and Hansen's CFD computational results supply an extensive database for the possible validations on various aspects of the theoretical model. Particularly, for the one-dimensional momentum theory discussed in the following sections in which the detailed form of rotor is not considered too much, it is worth to note that the Hansen's data, which was obtained by implementing the Actuator Disc Model in the CFD simulation, gives a sound validation benchmark for this specific issue.

The motivation of the present work comes from the interest in trying to consummate the existing Jamieson's theoretical model, by bringing about more light into it through some necessary effort. In the following parts, the paper discusses the links between Jamieson's theory and the previous classical theory, compares the approximation methods for the effective energy diffuser efficiency of the DAWT system, improves the Glauert correction for the thrust coefficient in the turbulent wake state, and proposes an empirical model for prediction of the axial velocity profile and the diffuser axial induction distribution at the rotor plane.

## 2 Fundamental methodologies for the diffuser-augmented wind turbines

### *2.1 The Generalized Actuator Disc Theory*

The Generalized Actuator Disc Theory (GADT) was first proposed by Jamieson [10], and then discussed in Jamieson [11] and Jamieson [12]. It extends the existing ADT (Actuator Disc Theory) to a more general case of a shrouded wind turbine, through the introduction of a new axial induction factor $a_0$ which accounts for the geometry of the given diffuser. As shown in Fig. 1, for the generalized flow in the upstream side of the extracted plane, application of Bernoulli's equation leads to

$$p_0 + \frac{1}{2}\rho V_0^2 = p_1 + \frac{1}{2}\rho V_0^2 (1-a)^2 , \tag{1}$$

and for the downstream flow, similarly

$$p_1 - \Delta p + \frac{1}{2}\rho V_0^2 (1-a)^2 = p_0 + \frac{1}{2}\rho V_0^2 \left[1 - f(a)\right]^2 \tag{2}$$

where $f(a)$ is assumed as the axial induction in the far wake. On the other hand, consider the relation between the pressure variations at any plane with the thrust coefficient

$$C_{\mathrm{T,d}} = \frac{2\Delta p}{\rho V_0^2} . \tag{3}$$

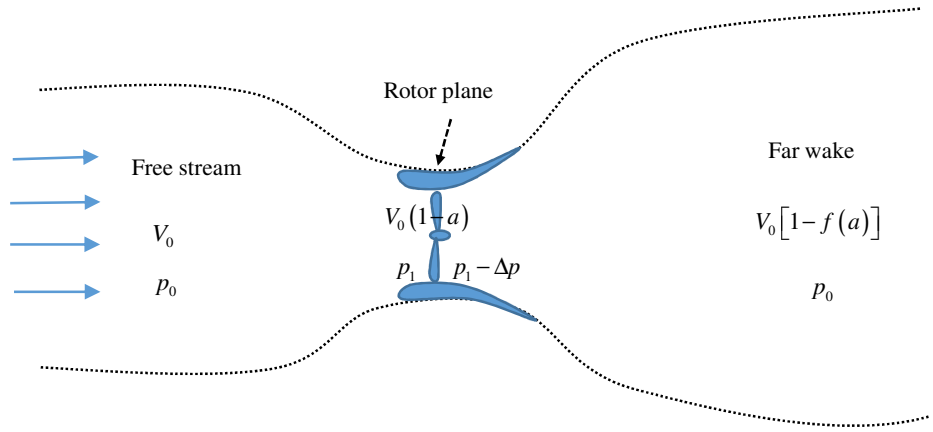


Fig. 1 Sketch of the diffuser-augmented wind turbine system

Combination of Eqs. (1) ~ (3) leads to the relation of the thrust coefficient with the axial induction in the far wake

$$C_{\mathrm{T,d}} = f(a)\left[2 - f(a)\right] . \tag{4}$$

The function $f(a)$ is unknown, but restricted to the following three conditions: (1) in the absence of energy extraction, $a = a_0$, and $f(a) = 0$; (2) when the flow is fully blocked, $a = 1$, and $C_{\mathrm{T,d}} = 0$; (3) in the presence of the rotor, since energy is extracted out from the system, the velocity in the far wake must be less than the ambient, i.e., $f(a) > 0$ for $a > a_0$. Solution of Eq. (4) therefore becomes

$$f(a) = \frac{2(a - a_0)}{1 - a_0}, \tag{5}$$

and

$$C_{\mathrm{T,d}} = \frac{4(a - a_0)(1 - a)}{(1 - a_0)^2}. \tag{6}$$

Since the power coefficient $C_{\mathrm{P,d}}$ has a relation with $C_{\mathrm{T,d}}$

$$C_{\mathrm{P,d}} = (1 - a) C_{\mathrm{T,d}}, \tag{7}$$

We have

$$C_{\mathrm{P,d}} = \frac{4(a - a_0)(1 - a)^2}{(1 - a_0)^2}. \tag{8}$$

Differentiating Eq. (8) with respect to $a$ determines the maximum power coefficient

$$C_{\mathrm{P,d}}^{\max} = \frac{8}{9}(1 - a_{\mathrm{m}}) \tag{9}$$

at $a = a_{\mathrm{m}}$ where

$$a_{\mathrm{m}} = \frac{1 + 2a_0}{3}. \tag{10}$$

The corresponding thrust coefficient matched with maximum energy extraction (optimal rotor loading) is

$$C_{\mathrm{T,d}}^{\mathrm{opt}} = \frac{8}{9}. \tag{11}$$

*2.2 The classical theory for shrouded wind turbines*

The classical DAWT theory has been developed through a much longer time history. Derivation of the formulation in detail can be found in many previous works (Fletcher [6]; Hansen et al. [8]; Rio Vaz et al. [13]). In this theory, the momentum equation keeps a consistent form with the classical

theory without diffuser. It introduces the diffuser velocity speed-up ratio $\gamma$ as its key part to account for the shrouding effect. In order to distinguish from the definition of $a$ that is used by Jamieson's theory, herein we use $b$ to express the axial induction factor. The critical difference between them is that $a$ represents the induction at the rotor plane, whereas $b$ represents the induction at the downstream far wake. The velocity speed-up ratio $\varepsilon$ is defined as the ratio of the flow velocity at the rotor plane to the free-stream velocity

$$\varepsilon = \frac{V_1}{V_0}, \tag{12}$$

which can be also written in an alternative way as the product of diffuser augmentation and loss of rotor blockage

$$\varepsilon = \gamma(1-b). \tag{13}$$

The thrust coefficient and power coefficient are

$$C_{\mathrm{T,d}} = 4b(1-b) \tag{14}$$

and

$$C_{\mathrm{P,d}} = \gamma 4b(1-b)^2, \tag{15}$$

respectively. Notice that Eqs. (14) and (15) also hold for the bare-rotor thrust coefficient $C_{\mathrm{T,b}}$ and the power coefficient $C_{\mathrm{P,b}}$ when $\gamma$= 1. In addition, from Eqs. (14) and (15) we obtain

$$C_{\mathrm{P,d}} = \varepsilon C_{\mathrm{T,d}}. \tag{16}$$

*2.3 Finding links between the two momentum theories*

In the classical DAWT theory, it is well-known that the downstream velocity in the far wake is

$$V_2 = (1-2b)V_0. \tag{17}$$

Comparing with Jamieson's theory it can be found that $b$ is equivalent to the half of induction in the far wake

$$b = \frac{a - a_0}{1 - a_0}, \tag{18}$$

which shows that $b$ involves the effect of diffuser.

On the other hand, according to the definition of Hansen et al. [8] and Jamieson [11], the diffuser velocity speed-up ratio can be expressed by

$$\gamma = 1 - a_0 . \tag{19}$$

Therefore, considering Eqs. (13), (18) and (19), we obtain

$$\varepsilon = (1 - a_0)\left(1 - \frac{a - a_0}{1 - a_0}\right) = 1 - a . \tag{20}$$

Since 1 - $a$ is exactly the ratio of rotor-plane flow velocity to the free-stream velocity that is defined in Jamieson's theory, which coincides with the definition of $\varepsilon$ defined in the classical theory with diffuser, Eq. (20) proves the consistence between the two theories.

As pointed out by Hansen et al. [8], the relative increase in the power coefficient for a diffuser-augmented wind turbine is proportional to the ratio of mass flow through the same rotor with and without the diffuser

$$\frac{C_{\mathrm{P,d}}}{C_{\mathrm{P,b}}} = \frac{\dot{m}_d}{\dot{m}_b} = \frac{\varepsilon}{1 - b} . \tag{21}$$

Combination of Eqs. (13), (19) and (21) leads to

$$\frac{C_{\mathrm{P,d}}}{C_{\mathrm{P,b}}} = \frac{\dot{m}_d}{\dot{m}_b} = 1 - a_0 . \tag{22}$$

This result shows the ratio of power coefficient between the shrouded and the non-shrouded turbine under the same thrust loading depends on the diffuser axial induction factor $a_0$, which relies on the given geometry of the diffuser.

## 3 Effective diffuser efficiency for evaluation of the turbine performance

The diffuser is not ideal if its maximum power coefficient does not occur at optimal rotor loading. This imperfection can be measured by a variable function which is called 'effective diffuser efficiency', approximating how closely the efficiency of the present diffuser at current status approaches the optimal performance of its initial design (Jamieson [11]). Consider a real diffuser system under non-optimum loading, and assume the effective diffuser efficiency to be a function of the axial induction factor

$$\eta(a) = \frac{C_{\mathrm{T,d}}(a)}{C_{\mathrm{T,d}}^{\mathrm{opt}}}, \tag{23}$$

the diffuser axial induction is actually not $a_0$, but $a_0\eta(a)$. The expressions for the thrust coefficient and the power coefficient therefore need to be improved by a slight modification on the axial induction factor, which can be re-expressed as

$$C_{\mathrm{T,d}} = \frac{4\left[a - a_0\eta(a)\right](1-a)}{(1-a_0)^2}, \tag{24}$$

and

$$C_{\mathrm{P,d}} = \frac{4\left[a - a_0\eta(a)\right](1-a)^2}{(1-a_0)^2}. \tag{25}$$

It should be noticed that the function $\eta(a)$ here is not always constant with respect to $a$, since it has been pointed out by Jamieson [11] that the constant effective diffuser efficiency is strictly valid only

at the critical condition where $C_{P,d}$ is maximum. Additionally, the ratio of mass flow between the shrouded and the non-shrouded turbine can also be re-expressed as

$$\frac{C_{P,d}}{C_{P,b}} = \frac{\dot{m}_d}{\dot{m}_b} = (1 - a_0)\eta(a) \cdot \tag{26}$$

Eq. (26) is very useful for calculating the effective diffuser efficiency under different thrust loading. In the meantime, solution for $a$ from Eq. (24) is

$$a = \frac{1}{2}\left\{\left[1 + a_0\eta(a)\right] - \sqrt{\left[1 - a_0\eta(a)\right]^2 - (1 - a_0)^2 C_{T,d}}\right\}, \tag{27}$$

which can be used to calculate $a$ if the relationship between $\eta(a)$ and $C_{T,d}$ is known.

However, the exact form of the variable function $\eta(a)$ is usually unknown beforehand. Jamieson [11] proposed a linear approximation in $a$ which can be written as

$$\eta(a) = \frac{a\left(1 - \eta_{pmax}\right) - a_m + a_0\eta_{pmax}}{a_0 - a_m}, \tag{28}$$

where $a_m$ is modified into

$$a_m = \frac{1 + 2a_0\eta_{pmax}}{3} \tag{29}$$

and $\eta_{pmax} = \eta(a_{pmax})$ represents the effective diffuser efficiency at power maximum point, which is also defined as the 'diffuser efficiency' in Jamieson's formulation.

Hansen's CFD results (Ref. [8]) provide a good source for verifying the above theory. In his work, the diffuser was made by deforming a NACA0015 airfoil. According to his quotation, for zero thrust loading, the ratio of the flow velocity at the rotor plane to the free-stream velocity is $\gamma$= 1.83, which means in the rotor absent state, $a_0$ = - 0.83. Besides, its maximum power coefficient occurs at $C_{T,d}$ = 0.8 indicating that the diffuser efficiency is 0.9 based on Eq. (23), as pointed out by Jamieson [11].

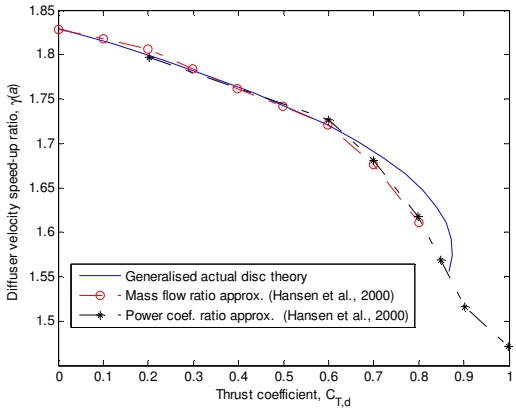


Fig. 2 Verification of theoretical results with CFD for the diffuser velocity speed-up ratio

Hansen et al. [8] supplies the $C_P$ -$C_T$ curve (including data for both shrouded rotor and non-shrouded rotor) and the $\eta$ - $C_T$ curve, which can both be used to calculate the diffuser velocity speed-up ratio and further the effective diffuser efficiency, through Eq. (26). Theoretical prediction of $\gamma$- $C_T$ relation by Eq. (24) coincides very well with that obtained from the CFD data when $C_T$ is less than 0.6, as shown in Fig. 2, which validates Eq. (24) when $C_T$ is small. The inconsistence for $C_T$ above 0.6 is caused by the turbulent wake state, where usually a Glauert-like correction should be used to eliminate the discrepancy. In the meantime, Fig. 2 confirms the validity of Eq. (23), since the $\gamma$- $C_T$ relations obtained from the mass flow ratio approximation and the power coefficient approximation seem to be equivalent.

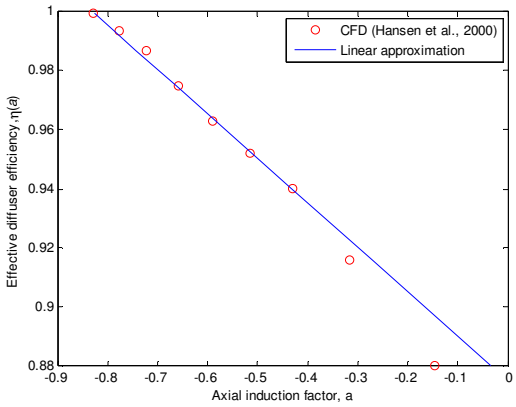

Fig. 3 Linear approximation for the effective diffuser efficiency

Fig. 3 compares the linear approximation based on Eq. (28) with the CFD data for prediction of the $\eta$ - $a$ relation. It can be observed that the linear formula provides a good approximation especially for the range $\eta$ >0.94.

## 4 Extended Glauert correction to the DAWTs in turbulent wake state

Similar to the ADT for the bare rotor in open flow, the GADT for the shrouded rotor in constrained flow needs a Glauert correction as well when the rotor approaches the turbulent wake state. In Section 3, the discrepancy between the theoretical and the computational results is found at about $C_T = 0.6$. In the extreme case that the DAWT system works always at optimal status for all the thrust loading, substituting Eq. (18) into Eq. (14) leads to the Eq. (6), which means the two formulations are equivalent. The half far-wake induction $b$ defined by Eq. (18) thus can be used as a basic variable for Glauert correction, as that has been done to $a$ in the open flow ADT. Consider the general case when there exists an effective diffuser efficiency for the DAWT system, substitution of the generalized version of Eq. (18) into Eq. (14) does not certainly lead to Eq. (24). The resulting expression of the thrust coefficient is therefore

$$C_{T,d} = \frac{4\left[a - a_0\eta(a)\right]\left\{1 - a + \left[\eta(a) - 1\right]a_0\right\}}{\left(1 - a_0\right)^2}. \tag{30}$$

Subtracting Eq. (24) from Eq. (30) and taking into consideration the linear $\eta$ - $a$ relation Eq. (28), difference between the two expressions can be written as

$$\Delta C_{T,d} = -\frac{4}{3}\frac{\left[1 - \eta(a)\right]^2\left(1 - a_0\eta_{pmax}\right)a_0}{\left(1 - \eta_{pmax}\right)\left(1 - a_0\right)^2}. \tag{31}$$

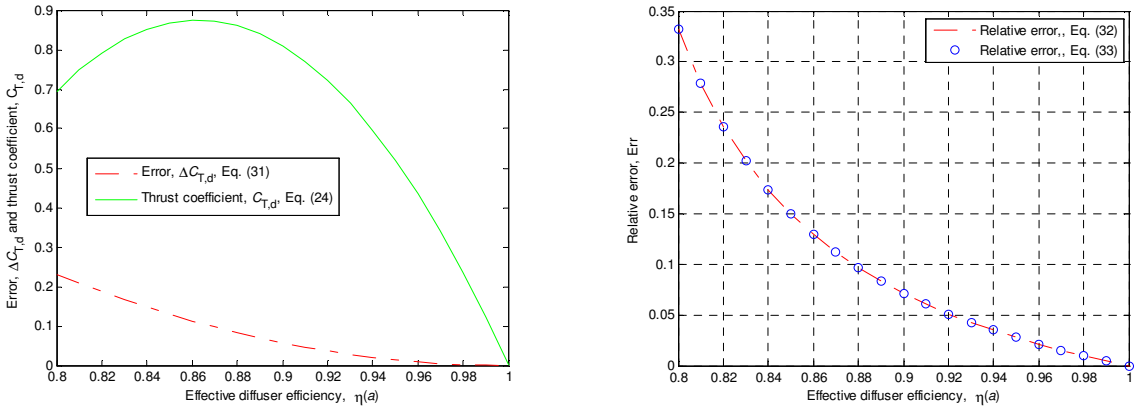


(a) absolute error (b) relative error

Fig. 4 Error estimation for the substitution of Eq.(30) for Eq.(24)

Ratio of Eq. (31) to Eq. (24) gives the relative error

$$Err = \left| \frac{\Delta C_{\mathrm{T,d}}}{C_{\mathrm{T,d}}} \right| = -\frac{1}{3} \frac{\left[1-\eta(a)\right]^2 \left(1-a_0\eta_{\mathrm{pmax}}\right) a_0}{\left(1-\eta_{\mathrm{pmax}}\right)\left[a-a_0\eta(a)\right](1-a)}, \tag{32}$$

which could also be given directly based on the difference between Eq. (30) and Eq. (24)

$$Err = \left| \frac{\Delta C_{\mathrm{T,d}}}{C_{\mathrm{T,d}}} \right| = \frac{\left[\eta(a)-1\right] a_0}{1-a}. \tag{33}$$

Fig. 4 shows the error estimation of employing the half far-wake induction $b$ as the variable in the thrust coefficient formulation Eq. (14), as that is done in open flow condition. It is evident from Fig. 4(a) that the absolute error for the thrust coefficient decreases with the increase of the effective diffuser efficiency. Fig. 4(b) is the local magnification of the relative error when $\eta$ becomes large, from which it is seen that the relative error is less than 5% for the region $\eta > \eta_c = 0.937$, where we define $\eta_c$ as the "cut-off point" between the ordinary thrust coefficient equation and the Glauert correction. Through Eq. (28) and the generalized version of Eq. (18), the corresponding values of the axial induction and the half far-wake induction at the cut-off point can be calculated out as $a_c$ =-0.412

231 and $b_c = 0.2$. Similar process can be performed to the values at the power maximum point. The results
232 are listed in Table 1.

233 Table 1. Calculated values at the two key points

| | $a$ | $b$ | $\eta$ | $C_{\mathrm{T,d}}$ | $C_{\mathrm{P,d}}$ |
|---|---|---|---|---|---|
| cut-off point | -0.4118 | 0.2000 | 0.9371 | 0.6172 | 0.8714 |
| maximum power point | -0.1788 | 0.3105 | 0.9000 | 0.8000 | 0.9431 |

234

235 For the Glauert correction, Jamieson [12] gives the formula, which is also used in the DNV GL's
236 commercial BEM software *Bladed*:

237
$$C_{\mathrm{T,d}}(a) = \begin{cases} \dfrac{4\left[a - a_0\eta(a)\right](1-a)}{(1-a_0)^2} \\ \quad for \;\; 0 \le a \le a_0 + 0.3539(1-a_0) \\ 0.6 + 0.61\left[\dfrac{a - a_0\eta(a)}{1-a_0}\right] + 0.79\left[\dfrac{a - a_0\eta(a)}{1-a_0}\right]^2 \\ \quad for \;\; a_0 + 0.3539(1-a_0) < a \le 1 \end{cases}, \tag{34}$$

238 where the result is shown in Fig. 5. Since the two curves has been detached from each other, it is
239 necessary to make them connected. The detachment of the two curves is partly due to the cut-off point
240 occurring at $b_c = 0.3539$, which can be obviously seen in Eq. (34). Therefore it is better to move the
241 cut-off point forward. We choose $b_c = 0.2$ in our following formulations.

242 Generally, the 'artificial' Glauert correction can be made by a polynomial function with any order
243 for the dependent variable, as long as the accuracy is satisfactory within prescribed tolerance range.
244 Although, the linear form is the simplest, it may be very helpful in practical engineering issues. We
245 choose the values at the optimal point $\left(b_{\mathrm{pmax}}, C_{\mathrm{T,d}}^{\mathrm{pmax}}\right)$ and the cut-off point $\left(b_c, C_{\mathrm{T,d}}^{c}\right)$ to determine the
246 linear equation of the straight line

247 $$C_{\mathrm{T,d}}(b)-C_{\mathrm{T,d}}^{\mathrm{pmax}}=\frac{C_{\mathrm{T,d}}^{\mathrm{pmax}}-C_{\mathrm{T,d}}^{c}}{b_{\mathrm{pmax}}-b_{c}}\left(b-b_{\mathrm{pmax}}\right). \tag{35}$$

248 where $b_{\mathrm{pmax}}=\frac{a_{\mathrm{pmax}}-a_0\eta_{\mathrm{pmax}}}{1-a_0}$ and $b_c=\frac{a_c-a_0\eta_c}{1-a_0}$. In the present case, the equation finally leads to the

249 linear Glauert correction

250 $$C_{\mathrm{T,d}}(a)=\begin{cases}4\left[\frac{a-a_0\eta(a)}{1-a_0}\right]\left[1-\frac{a-a_0\eta(a)}{1-a_0}\right] \\ \quad for\ \ a_0\le a\le a_0+0.2(1-a_0) \\ 0.3504+1.4482\left[\frac{a-a_0\eta(a)}{1-a_0}\right] \\ \quad for\ \ a_0+0.2(1-a_0)<a\le 1\end{cases}. \tag{36}$$

251 A second alternative choice is to apply quadratic polynomials for the thrust equation in the
252 turbulent state. The method of Marshall (2005) can be used, which applies the continuity condition
253 for the function value and the function derivative value at the cut-off point, and the continuity
254 condition for the function value at the optimal point. However, Marshall (2005)'s method will lead to
255 an apparent gap between the resulting Glauert correction curve and Hansen's CFD data especially
256 when $C_{\mathrm{T,d}}$ is large. Here we give one of the quadratic polynomial that better fit the CFD data as below

257 $$C_{\mathrm{T,d}}(a)=\begin{cases}4\left[\frac{a-a_0\eta(a)}{1-a_0}\right]\left[1-\frac{a-a_0\eta(a)}{1-a_0}\right] \\ \quad for\ \ a_0\le a\le a_0+0.2(1-a_0) \\ 0.5632+0.1815\left[\frac{a-a_0\eta(a)}{1-a_0}\right] \\ +0.9602\left[\frac{a-a_0\eta(a)}{1-a_0}\right]^2 \\ \quad for\ \ a_0+0.2(1-a_0)<a\le 1\end{cases}. \tag{37}$$

258 Fig. 5 shows comparison of the different schemes for the Glauert correction of the DAWT system.
259 The form of Eq. (30) for the normal thrust equation agrees well with the scattered CFD data in the
260 region of $\eta\ge\eta_c$. The error for the substitution of Eq. (24) is acceptable, as discussed in Fig. 4. In the

region of $\eta < \eta_c$, *Bladed*'s Glauert correction seems to have a bit larger distance to the scattered points, while the linear Glauert correction and the quadratic Glauert correction proposed in this paper behaves better.

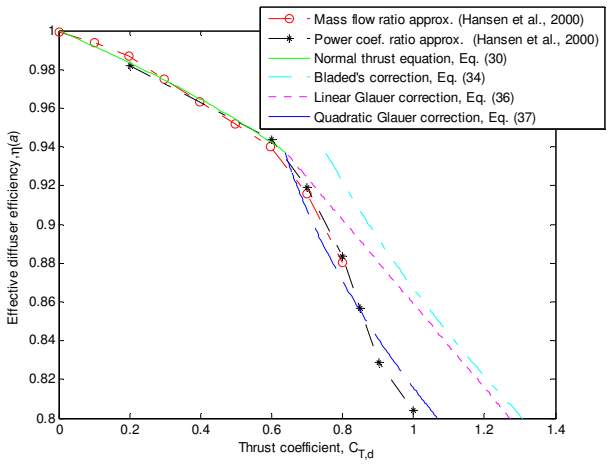


Fig. 5 Comparison of various schemes of Glauert correction

## 5 Prediction of the axial velocity profile at the rotor plane

In the GADT argued above, a physical parameter, i.e., the diffuser axial induction $a_0$, which is also related to the velocity speed-up ratio $\varepsilon$ at the rotor plane, plays the most important role. Through the introduction of this parameter, all the mathematical modelling becomes possible. Measurement or computation of the parameters $a_0$ or $\varepsilon$ needs a large amount of labour force and economical expense. It is better to develop an empirical method instead that can predict these parameters accurately, with sufficient validation.

Normally, to determine the diffuser axial induction $a_0$, the wind velocity profile at the rotor plane needs to be known in advance. This comes to the velocity speed-up ratio $\varepsilon$, since it is defined as the augmentation of flow velocity at the rotor plane. As revealed by Eq. (13), the velocity speed-up ratio under an arbitrary thrust loading can be decomposed into two factors, the diffuser velocity speed-up ratio $\gamma$ and the factor involving rotor axial induction (1- $b$). Particularly, in the extreme case of zero

thrust loading, the factor (1- $b$) vanishes, leading to $\varepsilon = \gamma = 1 - a_0$, which indicates the diffuser axial induction $a_0$ can be determined, as long as the distribution of the velocity ratio $\varepsilon$, which is also named as the axial velocity profile, is provided.

Due to the effect of diffuser, the axial velocity has an initial profile under zero thrust loading, which is speeded up most obviously in the region close to the diffuser wall, and decreases to the centre of the rotor disc. With the action of thrust force on the disc, the initial speeding up is counteracted by the axial induction from the rotor, and becomes increasingly weaker and weaker, until it is completely cancelled out and reversed by the rotor induction. Based on this mechanism, taking into consideration the similar tip-loss model in the BEM methodology, we suppose the following formula for the axial velocity profile with respect to the thrust loading and the radial location:

$$\varepsilon = p - \frac{2}{\pi}\cos^{-1}\left(e^{-f}\right) \tag{38}$$

and

$$f = \frac{g}{2}\frac{R-r}{R}\ , \tag{39}$$

where $g$ and $p$ are two parameters that can be determined by linear approximations

$$g = \left(\frac{g_1 - g_0}{C_{\mathrm{T,d}}^1 - C_{\mathrm{T,d}}^0}\right)\left(C_{\mathrm{T,d}} - C_{\mathrm{T,d}}^0\right) + g_0\ , \tag{40}$$

and

$$p = \left(\frac{p_1 - p_0}{C_{\mathrm{T,d}}^1 - C_{\mathrm{T,d}}^0}\right)\left(C_{\mathrm{T,d}} - C_{\mathrm{T,d}}^0\right) + p_0\ , \tag{41}$$

where the subscript and the superscript ‘0’ denotes the situation under zero thrust loading, and ‘1’ denotes the situation under full thrust loading $C_{\mathrm{T,d}} = 1.0$. The quantities $g$ and $p$ are trying to describe the curvature and the maximum value of the velocity profile, respectively, which are induced by the

combined action from the diffuser augmentation and the thrust loading. The value of $g$ and $p$ in these two subscripts can be determined by the computed profile by CFD simulation under these two conditions.

In the numerical example of Hansen et al. [8], the data of two axial velocity profiles computed by CFD are provided. Through some simple test, we determine the parameters as $g_0 = 0.3$, $g_1 = 0.01$, $p_0 = 2$ and $p_1 = 0.8$. Comparison for the approximated and the computed profiles is shown in Fig. 6. The two results agree very well with each other, which verifies that the present empirical model is quite helpful for prediction of the axial velocity profile under different thrust loadings.

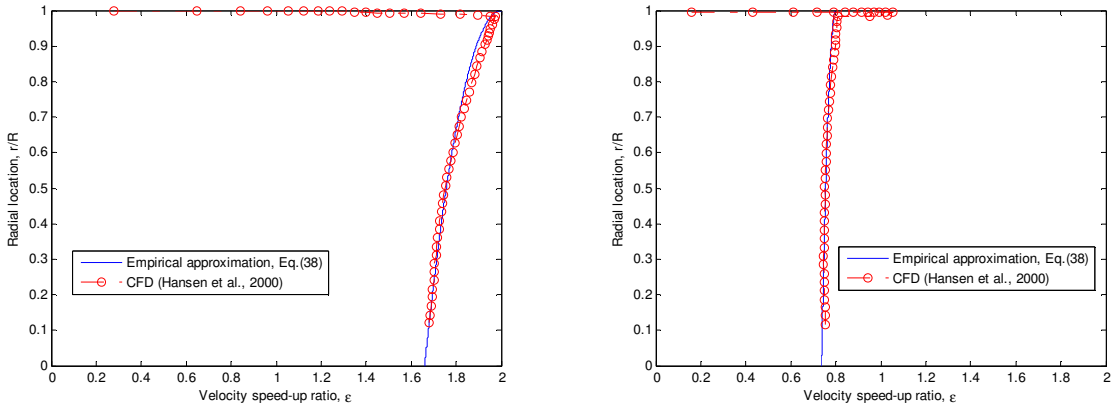


(a) $C_{T,d} = 0.0$ (b) $C_{T,d} = 1.0$

Fig. 6 Comparison of axial velocity profiles computed by the empirical model and CFD

The predicted axial velocity profile is essential to the determination of the velocity speed-up ratio and the diffuser axial induction at different radial locations. It provides important information for the input of the Generalized Blade Element Method (GBEM), in which the diffuser axial induction is required to be known at different radial locations beforehand. To calculate the averaged value of the diffuser velocity speed-up ratio $\gamma$and the diffuser axial induction $a_0$, we just need to simply compute the area bounded by the profile curve and the lines of $r/R = 0$ and $\varepsilon = 0$ in the condition $C_{T,d} = 0.0$, and then divided by one. Numerical integration of the surrounded area in Fig. 6(a) gives the

316 approximated result $\gamma$= 1.78, thus $a_0$ = 1- $\gamma$= -0.78. Comparing with the value given in Hansen et al.

317 [8], i.e., $a_0$ = -0.83, there is an absolute error 0.05 or a relative error 6.02%.

318 Since $\varepsilon$ > 1.0 when $C_{T,d}$ = 0.0, and $\varepsilon$ < 1.0 when $C_{T,d}$ = 1.0, there must be a value of $C_{T,d}$ under

319 which the velocity speed-up ratio $\varepsilon$ is equal to unity. As inferred from Eq. (20), at this loading

320 condition, the axial induction should be zero, which implies that the augmentation effect of the diffuser

321 is completely cancelled out by the induction effect of the rotor. Therefore, we define this loading as

322 'zero-induction thrust loading', also as 'critical thrust loading'. Fig. 7 shows prediction of the axial

323 velocity profile under the critical thrust loading $C_{T,d}^{cr}$. Again, through the similar technique, integration

324 gives the averaged value of the velocity speed-up ratio $\varepsilon$ = 0.953, which approximately approaches

325 unity, with an absolute error 0.047 or a relative error 4.7%.

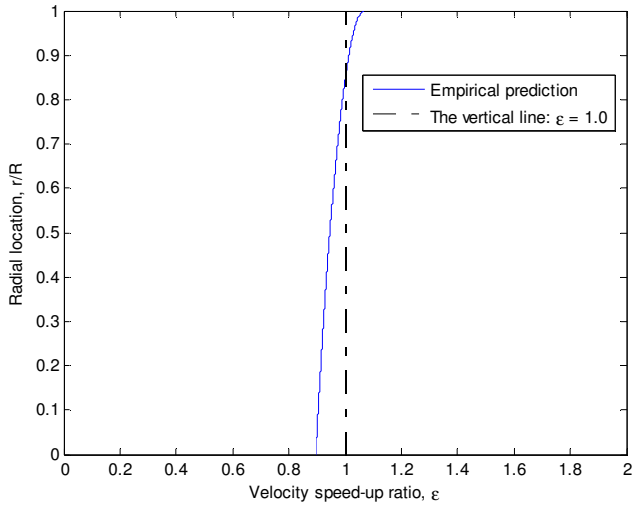


326

327 Fig. 7 Prediction of the axial velocity profiles under the critical thrust loading

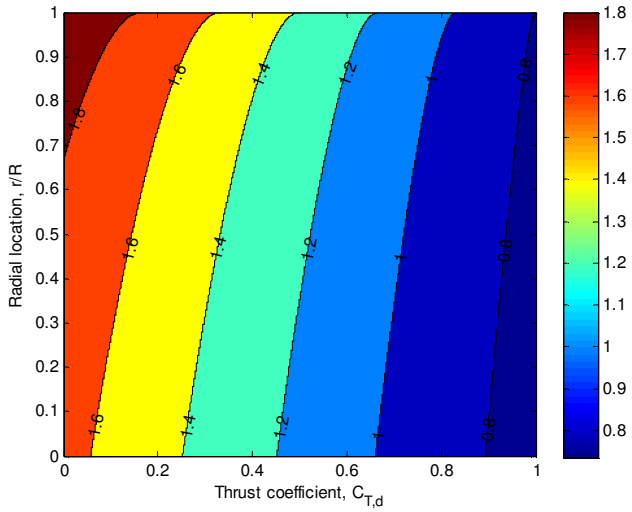


328

329 Fig. 8 Distribution of the velocity speed-up ratio at various thrust loadings and radial locations

330 Fig. 8 shows the contour plot of the velocity speed-up ratio under various thrust loadings and at
331 different radial locations. It can be evidently seen that, the smaller the thrust loading is and the larger
332 the radial distance is, the larger the velocity speed-up ratio will be. The largest velocity speed-up ratio
333 occurs in the region near the point $C_{T,d}$ = 0.0 and $r/R$ = 1.0, and the smallest velocity speed-up ratio
334 occurs at the region near the point $C_{T,d}$ = 1.0 and $r/R$ = 0.0. The visual result is reasonable by
335 contrasting to the CFD profile given in Hansen et al. [8].

336 **Conclusions**

337 The GADT that first brought forth by Jamieson ([10], [11]) helps a lot in revealing the physical
338 mechanism for the diffuser-augmented wind turbine behind the phenomena. It can be better
339 understood through taking into consideration simultaneously the classical theory for shrouded wind
340 turbine. The present work tries to dig more deeply in the GADT, including the following aspects:

341 (1) Links between the GADT and the classical DAWT theory has been argued, especially the
342 relation between the axial induction and the velocity speed-up ratio.

(2) Jamieson's linear approximation formulation for the effective diffuser efficiency has been compared with Hansen's CFD data, showing that it works pretty well especially in the high diffuser efficiency range.

(3) Glauert corrections for the DAWT are studied. A linear and a quadratic approximation formulae have been proposed. Validation is given by comparing with Jamieson's formula and Hansen's CFD data.

(4) The GADT is further extended to include approximation of the axial velocity profile by establishing an empirical model, which is essential to the prediction of the diffuser axial induction. Comparison between the CFD results justifies the effectiveness of the present model.

It should be noticed that at the current stage, the above GADT is still necessary to be applied with the assist of the CFD method, particularly for the determination of its several important parameters. In addition, the empirical model for predicting the axial velocity profile still cannot explain the small gap close to the region between the blade tip and the boundary layer of the diffuser wall, which should be further improved as a future work.

## Acknowledgements

All the authors gratefully appreciate the valuable discussions with Prof. Jamieson in the past research. The first author gratefully acknowledges the financial support provided by the MEXT Scholarship (Grant No. 123471) from Japanese Government during the three-year PhD research.

## References

[1] N. Oka, M. Furukawa, K. Yamada, K. Kawamitsu, K. Kido, A. Oka, Aerodynamic Design Optimization of Wind-lens Turbine. EWEA 2014, Barcelona, Spain.

[2] W.J. Rainbird, G.M. Lilley, A Preliminary Report on the Design and Performance of a Ducted Windmill. (Report 102), College of Aeronautics Cranfield, 1956.

366 [3] B.L. Gilbert, K.M. Foreman, Fluid Dynamics of Diffuser-Augmented Wind Turbines. Journal of Energy
367 1978; 2(6): 368 – 374.

368 [4] B.L. Gilbert, K.M. Foreman, Experimental Demonstration of the Diffuser-Augmented Wind Turbine
369 Concept. Journal of Energy 1979; 3(4): 235 – 240.

370 [5] O. Igra, Research and development for shrouded wind turbines. Energy Convers Manage 1981; 21:13–48.

371 [6] C.A. Fletcher, Computational analysis of diffuser-augmented wind turbines. Energy Convers Manage 1981;
372 21:175–83.

373 [7] E. Dick, Momentum analysis of wind energy concentrator systems. Energy Convers Manage 1984; 24:19–
374 25.

375 [8] M.O.L. Hansen, N.N. Sorensen, R.G.J. Flay, Effect of placing a diffuser around a wind turbine. Wind Energy
376 2000; 3:207–213.

377 [9] G.J.W. Van Bussel, The science of making more torque from wind: diffuser experiments and theory
378 revisited. Journal of Physics: Conference Series 2007; 75(1): 1–12.

379 [10] P. Jamieson, Generalized limits for energy extraction in a linear constant velocity flow field. Wind Energy
380 2008; 11: 445 – 457.

381 [11] P. Jamieson, Beating Betz - Energy Extraction Limits in a Uniform Flow Field. EWEC 2008, Brussels,
382 Belgium.

383 [12] P. Jamieson, Innovation in wind turbine design. John Wiley & Sons, 2011.

384 [13] D.A.T.D. Rio Vaz, A.L. Amarante Mesquita, J.R.P. Vaz, C.J.C. Blanco, J.T. Pinho, An extension of the
385 Blade Element Momentum method applied to Diffuser Augmented Wind Turbines. Energy Convers Manage
386 2014; 87:1116–1123.

387 [14] L.B.Jr. Marshall, A new empirical relationship between thrust coefficient and induction factor for the
388 turbulent windmill state. Technical report NREL/TP-500-36834, 2005.